µFLU14-82

KINETICS OF ANTIBODY RELEASE FROM GELATINE LAYERS FOR ON-CHIP SAMPLE PREPARATION

Xichen Zhang*[1], Dorothee Wasserberg[1], Leon W.M.M. Terstappen[1], Markus Beck[1]
[1]Department of Medical Cell Biophysics, University of Twente
Drienerlolaan 5, P.O. Box 217 Enschede, 7500 AE, The Netherlands
x.zhang-4@utwente.nl, d.wasserberg@utwente.nl, l.w.m.m.terstappen@utwente.nl, m.beck@utwente.nl

KEY WORDS

Controlled release, gelatine xerogel, point-of-care diagnostics

ABSTRACT

On-chip sample preparation is essential for an easy, robust and accurate operation of point-of-care (POC) diagnostic devices. We recently demonstrated a simple cell-counting device realised by controlled antibody release from a gelatine layer implemented on a microfluidic chip. However, little is known about the release kinetics from this gelatine layer with sub-micrometre(µm)-scale thickness. In this work, we have realised real-time and in situ monitoring of antibody release from sub-µm thick gelatine layers on second to minute timescale. The measured antibody release kinetics comply with diffusion controlled release. Release times between ~20 s and ~840 s are obtained from dry layers with the thicknesses between 0.25 µm and 1.5 µm. The estimated diffusion coefficient in equilibrium swelling gelatine layer is 0.4 µm^2/s. Higher drying temperatures result in a lower degree of physical crosslinking and further lead to shorter release time. In addition, we observe a considerably faster release from an inkjet-printed gelatine layer compared with the release from a cast layer prepared under comparable conditions. Moreover, the ionic strength of the medium is found to have a significant impact on release kinetics.

1. INTRODUCTION

Controlled reconstitution of anhydrous reagents integrated in microfluidic devices shows great potential in POC diagnostics for low-resource settings. First, the dependence of external instrumentation for precise reagent delivery into microfluidics is minimised. Second, the extensive bench top sample preparation is simplified[1]. Third, the reagent in its dry state is stable during both transport and long-term storage. The integration of anhydrous reagents in microfluidic devices has developed to pursue controlled release of reagents following rehydration for desired biochemical reactions. There are two strategies to achieve on-chip reagent release. One depends on the fabrication of sophisticated microfluidic chips.[2-5] The other strategy adopts a concept from drug delivery research by implementing a polymer matrix with embedded reagents in a microfluidic chip. Integrated polymer carriers, in the form of nanofibers[6] and microparticles[7], serve as matrices and their physiochemical properties enable controlled release of the reagents. Nevertheless, the preparation and integration of such polymer carriers still involve complexity. Thus, the development of a low-cost microfluidic device simply integrated with a polymer matrix would be a solution to realise on-chip reagent release for in vitro diagnostic applications.

We recently demonstrated on-chip sample preparation for the enumeration of CD4+ T-lymphocytes using cell counting chambers containing a dry gelatine layer in which fluorescently labelled antibodies are embedded.[8] In this concept, the release of antibodies following the filling of the chamber with whole blood is delayed by an approximately 150 nm thick gelatine layer. This delayed release is necessary to prevent

* Corresponding author

antibodies from being washed off by inflowing blood, thus ensure uniformity of cell staining and a high accuracy of the cell count.

To further optimise this concept and broaden its range of applications with other reagents, a fundamental understanding of the release kinetics is essential. Conventional drug delivery studies generally focus on long-term release on the timescale of hours to days from polymer layers of tens of µm to mm thick.[9, 10] Microfluidics applications generally require thinner layers and shorter release times. For our application, gelatine layers with sub-µm-scale thickness was used to release fluorescently labelled antibodies within the required timescale (seconds to minutes). Few research papers have reported release kinetics from such thin layers or on such short timescale.[11]

Therefore, we have realised real-time and *in situ* monitoring of release processes in microfluidic chips and studied the influence of various parameters on the release kinetics. Parameters are layer thickness, drying temperature, ionic strength of the medium and layer preparation method. In the release experiments, the medium passes through a fluidic chamber containing the dry gelatine layer embedding fluorescently labelled antibodies. This process mimics the filling of the cell counting chamber with blood. We analyse the fluorescence decrease from the layer during the release process using a custom-built fluorescence imaging setup. The layers are prepared by either casting a small volume of gelatine/antibody solution into the centre of the fluidic chamber or by dispensing gelatine/antibody solution using an inkjet printer. From cast layers, the measured kinetics fit well with diffusion controlled release. Both drying temperature and ionic strength of the medium strongly influence the release kinetics. Printed layers display a much faster release than cast layers.

To the best of our knowledge, this is the first study of controlled release from sub-µm thick gelatine layers with a time resolution of a few seconds. Understanding the release mechanism in microfluidic chips would be beneficial to help tailor reagent release kinetics and may expand the applications from the delayed release in our cell counting chambers to on-chip reagent release triggered by external stimuli.[12]

2. METHODS AND MATERIALS

2.1 Fluidic chip fabrication and sample coating

Fluidic chips were built from substrate slides (poly(methyl methacrylate)), laminating adhesive (nominal thickness 25.4 µm, 3M), gelatine (type A, Bloom No. 295, Sigma),antibody (Allophycocyanin conjugated antiCD3, clone SK7, BD Biosciences) solutions and capping slides (Menzel). The fluidic chamber (61 mm × 4.8 mm) was created by cutting laminating adhesive with a programmable cutting machine (Craft Robo, Graphtec) and attaching it to a substrate slide. Two coating procedures were applied as described below. After coating, a capping slide with two holes to connect tubing was attached to the adhesive, thus creating the chamber with a dry layer on the surface. Fig.1 shows the schematic of the fluidic chip. The assembled chips were stored dry at 4˚C until use.

2.1.1 Casting

Allophycocyanin conjugated antiCD3 (APC-αCD3) was diluted in 0.03% w/v gelatine solution to obtain a final concentration of 0.3 µg/ml. 3 µl of gelatine/APC-αCD3 solution was cast onto substrate slides within the fluidic chamber. The fluidic chamber was placed on a temperature-controlled heating stage. The solutions were dried at various temperatures to form circular gelatine/APC-αCD3 layers. Higher concentrations of gelatine solutions resulted in thicker layers.

2.1.2 Inkjet printing

The inkjet printing was performed using a printer (PiXDRO LP50, Roth&Rau) equipped with a piezo-actuated single nozzle dispenser (MicroFab). The nozzle dispensed 20 pl of gelatine/APC-αCD3 drops and the substrate was programmably shifted during jetting to provide proper inter-drop distance which prevent drop merging before drying. Full coverage of the surface and variation of the layer thickness was obtained by successive deposition of sub-layers with spatial offsets.

2.2 Fluorescence imaging for monitoring of antibody release

A custom-built fluorescence imaging setup[8] was used to measure the release kinetics. The excitation light from a red LED (Phlatlight CBT-40, Luminus Devices) passes a 650 nm short pass filter (Semrock) and is projected onto a gelatine/APC-αCD3 layer. The emitted fluorescence is collected using a close-up lens (LM-scope) filtered with a 685/40 nm band pass filter (Semrock) and recovered by CCD camera through a 60 mm macro-lens (AF Micro-Nikkor, Nikon).

Medium, either phosphate buffered saline (PBS) or micro-filtered deionised (DI) water, was flown through the fluidic chip at a rate of 1 μl/s, which is similar to the capillary flow of blood filling the cell-counting chambers, and fluorescence images were taken every 5 s with exposure time of 1 s. Fluorescence intensity against layer thickness and the amount of APC-αCD3 remaining in the layer were both calibrated. Regions of interest (ROIs) with predetermined initial thickness were selected and analysed for all successive images to study the release kinetics.

3. RESULTS AND DISCUSSION

3.1 Characterisation of cast and printed gelatine/APC-αCD3 layers

Fig.2 shows fluorescence images of dry gelatine/APC-αCD3 layers prepared by casting and inkjet printing. Gelatine and APC-αCD3 remain mixed during drying, the initial thickness of the dry layer is determined from the fluorescence intensity. The thickness profile of both cast and printed layers along the white line in Fig.2a and b is shown in Fig.2c. With respect to the cast layer, the thickness of the edge of the dry spot is approximately 5 times that of the interior. The presence of crystals in the dry layer is due to the salt residue in the gelatine/APC-αCD3 solution (Fig.2a). Crystalline region was excluded from image analysis. Regarding to the printed layer, thicker edge is not found in the profile. However, the overall layer is less smooth than the interior of the cast layer. Compared to the large volume (μl) of solution cast on a single spot, the printed layer is an orderd distribution of drops with small volume (pl). The roughness in the printed layer might be the compromised outcome of the similar thickness between the edge and the interior.

3.2 Cast layer thickness-dependence of release

Fig.3a shows the cumulative release of APC-αCD3 from cast gelatine layers with various initial thicknesses. The percentage of released antibody over total amount of antibody was calculated by comparing the APC-αCD3 released from the layer at a given time point (M_t) to the total APC-αCD3 embedded in the layer (M_{total}). All the data for the first 60% of APC-αCD3 release fit well with the Higuchi model[13]:

$$\frac{M_t}{M_{total}} = \left(\frac{t}{\tau}\right)^{1/2}, \tag{1}$$

The $t^{1/2}$ dependency is characteristic of Fickian diffusion, suggesting the release is diffusion controlled until 60% of APC-αCD3 is released.[14] τ is the release time and can be expressed as[15]:

$$\tau = \pi L^2 / 4D, \tag{2}$$

where D is the APC-αCD3 diffusion coefficient in the gelatine layer, and L is the thickness of the gelatine layer. From the power law dependence $M_t/M_{total} \propto t^{1/2}$, we can conclude that D/L^2 is constant during the first 60% of the release process. The dependence of the release times on the initial thicknesses of dry gelatine layers, plotted in Fig.3b, clearly shows that the release time is proportional to the square of the thickness of dry layer. We have determined an equilibrium swelling ratio of 13.5 in PBS. The layer we prepared has negligible thickness compared to its diameter, therefore the swelling develops in one-dimension and swelling ratio is the ratio of swelling thickness over initial thickness. According to equation (2), the calculated diffusion coefficient of APC-αCD3 in the equilibrium swelling gelatine layer is 0.40 $\mu m^2/s$, 2 orders of magnitude less than that in PBS[16], confirming the release is delayed by gelatine.

3.3 Influence of drying temperature on the release from cast layers

Gelatine/APC-αCD3 solutions were cast on the substrates at the temperatures of 27, 35 and 40˚C to create dry layers with average thickness of 500 nm. In Fig.4a, the layers dried at 40˚C substrate show the fastest

release kinetics with 36 s release time. Longer release times, 45 s and 87 s, were found for the layers dried at 35 and 27˚C, respectively. It has been reported that the structure of gelatine layers is strongly influenced by the drying conditions, in particular drying temperature.[17] Gelatine layers dried at room temperature or lower show ordered helical structure, these layers are called 'cold' films. In contrast, gelatine layers dried at 35˚C or above, called 'hot' films, have randomly coiled structure. Compared with amorphous 'hot' film, 'cold' film with ordered helical structure has higher degree of physical crosslinking to resist layer expansion and swelling.[18] Therefore, a constrained gelatine layer dried at 27˚C leads to a slow antibody diffusion.

3.4 Influence of ionic strength of the medium on the release from cast layers

PBS and DI water were compared to study the influence on the release of APC-αCD3 from cast gelatine layers. As shown in Fig.4b, the release time in PBS is much shorter than that in DI water and almost 50% of APC-αCD3 seems to be trapped in the layer immersed in DI water. Both gelatine and APC-αCD3 contain charged functional groups. The concentrated ions in PBS couple with those charged groups and shield the electrostatic interactions between gelatine and antibody, making antibody molecules easily detach from the gelatine matrix. Without the ion competition in DI water, stronger electrostatic interactions between gelatine and antibody induces a longer release time and less antibody release.

3.5 Comparison of release kinetics from cast layers and printed layers

Inkjet printing was employed to demonstrate the feasibility of fabricating cell-counting chambers using production techniques. The influence of the layer preparation method on the release kinetics was studied. Fig.5 compares the release from cast layers and printed layers with similar thickness. It turns out that the release from printed layer is much faster. The composition of small-volume drops in the printed layer probably reduces gelatine chain entanglement and further allows for faster water penetration and faster swelling. Conversely, the single spot with large volume in the cast layer provides complex entanglement, thus supporting a tightly connected network. Further studies are needed to reveal whether this structure change is caused by the shear forces during the jetting process.

4. FIGURES AND TABLES

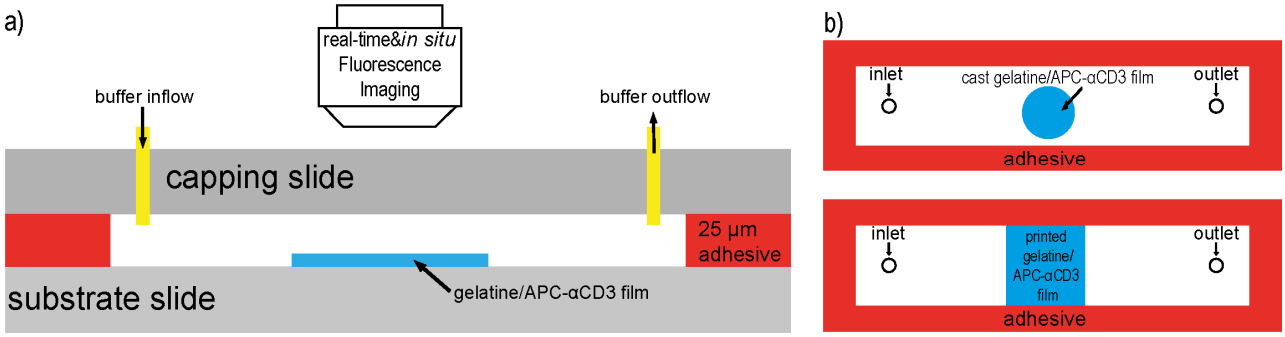

Figure 1: Schematic of the fluidic chip. a) side view. b) top views of cast and printed layers.

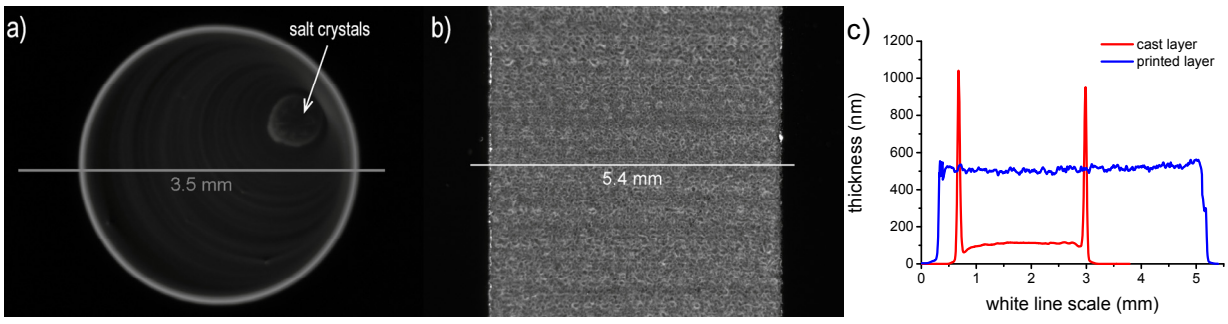

Figure 2: Fluorescence images a) cast layer and b) printed layer. c) The thickness profile of both cast and printed layers along the white lines.

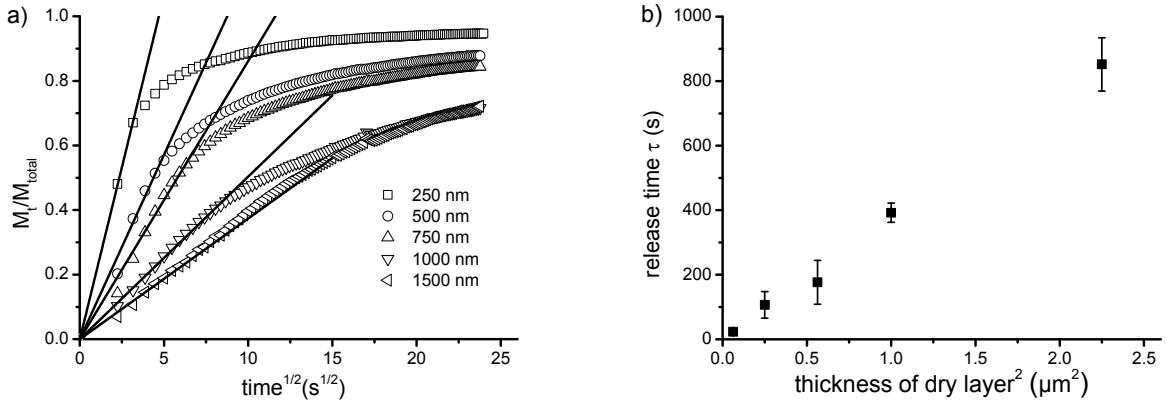

Figure 3: a) Measured release kinetics of APC-αCD3 from cast layers with various thicknesses fit to $M_t/M_{total}=(t/\tau)^{1/2}$ (solid line). b) The release time τ is proportional to the square of the thickness of dry layer.

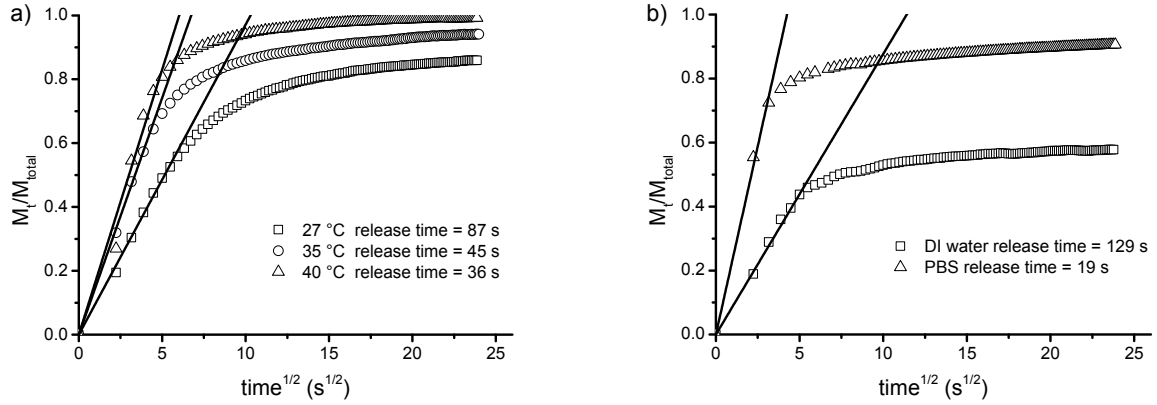

Figure 4: a) Measured release kinetics of APC-αCD3 from 500 nm thick layers dried at various temperatures fit to $M_t/M_{total}=(t/\tau)^{1/2}$ (solid line). b) Measured release kinetics of APC-αCD3 from 170 nm thick layers in DI water and PBS fit to $M_t/M_{total}=(t/\tau)^{1/2}$ (solid line).

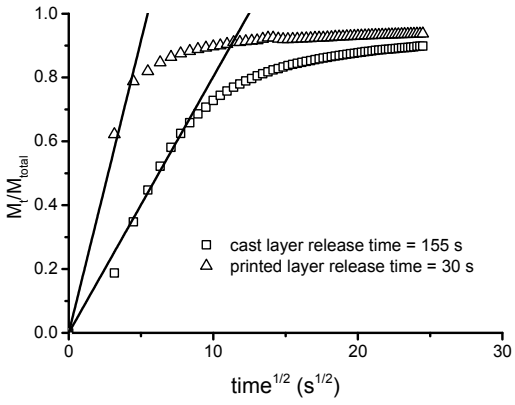

Figure 5: Comparison of APC-αCD3 release from the cast layer and printed layer. Both layers are 500 nm thick.

5. CONCLUSIONS

In conclusion, we have studied the release kinetics of antibody embedded in a gelatine layer with sub-μm-scale thickness on second to minute timescale. Both cast and inkjet-printed gelatine layers were monitored by

real-time and *in situ* fluorescence imaging during the release in a flow setup. The observed first 60% of antibody release from cast layers is proportional to $t^{1/2}$, as expected for diffusion controlled release. Also, the dependence of the release time on the thickness of the dry layer indicates a diffusion controlled process. Drying temperature and medium ionic strength have significant impact on release kinetics. Much faster release is observed from printed layers. A deeper understanding of this release mechanism would help to address the challenge of reagent and sample mixing in microfluidic chips.

ACKNOWLEDGEMENTS

This work was funded by the European Research Council ERC under grant number 282276.

REFERENCES AND CITATIONS

[1] Chan, S. D. H., et al. (2003). Cytometric analysis of protein expression and apoptosis in human primary cells with a novel microfluidic chip-based system. *Cytometry Part A*, **55A**(2): 119-125.
[2] Focke, M., et al. (2010). Centrifugal microfluidic system for primary amplification and secondary real-time PCR. *Lab on a Chip*, **10**(23): 3210-2.
[3] Hitzbleck, M., Gervais, L., & Delamarche, E. (2011). Controlled release of reagents in capillary-driven microfluidics using reagent integrators. *Lab on a Chip*, **11**(16): 2680-2685.
[4] Lee, B. S., et al. (2009). A fully automated immunoassay from whole blood on a disc. *Lab on a Chip*, **9**(11): 1548-55.
[5] Lutz, S., et al. (2010). Microfluidic lab-on-a-foil for nucleic acid analysis based on isothermal recombinase polymerase amplification (RPA). *Lab on a Chip*, **10**(7): 887-893.
[6] Nagai, Y., et al. (2006). Slow release of molecules in self-assembling peptide nanofiber scaffold. *Journal of Controlled Release*, **115**(1): 18-25.
[7] An, H. Z., Helgeson, M. E., & Doyle, P. S. (2012). Nanoemulsion composite microgels for orthogonal encapsulation and release. *Adv Mater*, **24**(28): 3838-44.
[8] Beck, M., et al. (2012). On-chip sample preparation by controlled release of antibodies for simple CD4 counting. *Lab on a Chip*, **12**(1): 167-173.
[9] Dong, Z. F., Wang, Q., & Du, Y. M. (2006). Alginate/gelatin blend films and their properties for drug controlled release. *Journal of Membrane Science*, **280**(1-2): 37-44.
[10] Mandal, B. B., Mann, J. K., & Kundu, S. C. (2009). Silk fibroin/gelatin multilayered films as a model system for controlled drug release. *European Journal of Pharmaceutical Sciences*, **37**(2): 160-171.
[11] Zhan, W., Seong, G. H., & Crooks, R. M. (2002). Hydrogel-based microreactors as a functional component of microfluidic systems. *Analytical Chemistry*, **74**(18): 4647-4652.
[12] Mortato, M., et al. (2012). pH controlled staining of CD4(+) and CD19(+) cells within functionalized microfluidic channel. *Biomicrofluidics*, **6**(4).
[13] Higuchi, T. (1961). Rate of release of medicaments from ointment bases containing drugs in suspension. *J Pharm Sci*, **50**: 874-5.
[14] Siepmann, J., Lecomte, F., & Bodmeier, R. (1999). Diffusion-controlled drug delivery systems: calculation of the required composition to achieve desired release profiles. *Journal of Controlled Release*, **60**(2-3): 379-89.
[15] Siepmann, J., Siegel, R. A., & Rathbone, M. J. *Fundamentals and Applications of Controlled Release Drug Delivery*, ed. M. Rathbone, J. 2012.
[16] Schnell, E.A., et al. (2008). Diffusion measured by fluorescence recovery after photobleaching based on multiphoton excitation laser scanning microscopy. *J Biomed Opt*, **13**(6): 064037.
[17] Badii, F., et al. (2014). The effect of drying temperature on physical properties of thin gelatin films. *Drying Technology*, **32**(1): 30-39.
[18] Ofner, C. M., & Schott H. (1986). Swelling Studies of Gelatin .1. Gelatin without Additives. *Journal of Pharmaceutical Sciences*, **75**(8): 790-796.

